Impact of snow albedo parameterization when modelling Svalbard glaciers

SVALI DELIVERABLE D3.2-8

Report

BJÖRN CLAREMAR
SVALI POSTDOC
DEPARTMENT OF EARTH SCIENCES
UPPSALA UNIVERSITY, SWEDEN
&
PETRI RÄISÄNEN
FINNISH METEOROLOGICAL INSTITUTE
HELSINKI, FINLAND
JUNE/AUGUST 2015

UPPSALA UNIVERSITET

ABSTRACT

Albedo is of great importance in the surface energy balance. It affects surface skin temperature which in turn affects the atmospheric stratification and the temperature in the snow. For the snow, this affects the melting process and the snow mass balance. The snow metamorphosis may in turn affect the albedo to some degree and especially the timing of glacier surface exposure is of great importance. There is mainly a decrease in the albedo as the snow is aging after a snowfall. On longer time scale the summer melt increases the concentration of impurities and growth of algae further decreasing the albedo.

In this report simulations with the atmospheric model WRF are presented and analysed. First, the sensitivity and effect on albedo of changing snow grain shape in a high-order snow scheme is investigated. Second, the effect on snow and air temperature of fitting the albedo in a lower-order snow scheme to observations is studied. The observations include in-situ measurements at three sites on Svalbard glaciers with different surface mass balance properties as well as remote sensing data from MODIS satellite observations.

It is shown that different MODIS products give different albedos at the sites. The 1-day albedo was an average closer to the in-situ observations except on Lomonosovfonna where the 16-day albedo was closer.

The effect of grain shape on albedo is small but still significant on 2-m air temperature and snow temperature. It is not evident if an albedo treatment based on spherical snow grains or non-spherical grains (an optimized habit combination; OHC) results in better agreement with observations. In the higher-order scheme the surface snow is heated by penetrating short wave radiation that is absorbed by the snow. This is probably why the summer snow temperature is much higher in this scheme and why the lower-order snow scheme requires a high snow thermal conductivity to account for the sub-surface heating in the summer. Further work is required to capture the effect of snow aging on the albedo.

INTRODUCTION

Albedo is of great importance in the surface energy balance. It determines the part of the shortwave radiation that is reflected and hence also the part absorbed by the surface. The surface energy balance, with the radiation, turbulence and ground heat fluxes, all together, determines the surface skin temperature which in turn affects the atmospheric stratification and the temperature in the snow. For the snow, this affects the melting process and the snow mass balance (SMB). The snow metamorphosis may in turn affect the albedo and especially the timing of glacier surface exposure to the atmosphere and solar radiation is of great importance.

The broadband albedo can be divided into spectral band albedos taking into account the effect of different wavelengths. Snow albedo requires extra care compared to other surfaces because of the change of the snow properties with time. The albedo is affected by snow grain structure, dust and soot concentration, liquid water, among other properties, as well as the solar elevation and cloudiness (Oerlemans 2010). There is mainly a decrease in the albedo as the snow is aging after a snowfall and this process is relatively fast, with a decrease of 0.1 to 0.2 in a couple of days. On a longer time scale the summer melt increases the concentration of impurities and growth of algae further decreases the albedo.

While radiative transfer calculations involving snow often assume spherical snow grains, in reality snow grains are distinctly non-spherical. In a recent study, Räisänen et al. (2015) developed, based on angular scattering measurements for blowing snow, an optimized habit combination (OHC) for approximating the scattering by snow. The OHC consists of three non-spherical shapes: severely rough droxtals, aggregates of severely rough plates and strongly distorted Koch fractals. The main practical difference to spherical grains (which are used in the snow scheme SNICAR) is that a higher albedo is achieved, especially for the IR part of the spectrum.

In this report, simulations with the atmospheric model WRF are presented and analysed. The focus is two-fold. First, the sensitivity and effect on the albedo of changing snow grain shape in a high-order snow scheme (SNICAR) is investigated by changing table parameters connected to the grain shapes. Second, the effect of introducing maximum albedos from the SNICAR scheme into the simpler BATS scheme is investigated, along with the effect of changing the snow aging parameter. The simulations with WRF are compared with albedo observations. The observations are in-situ at three sites on Svalbard glaciers with different SMB properties as well as remote from MODIS satellite observations. Further the effect on the 2-m temperature and the snow temperature is investigated.

MODEL AND MEASUREMENTS

WRF Model

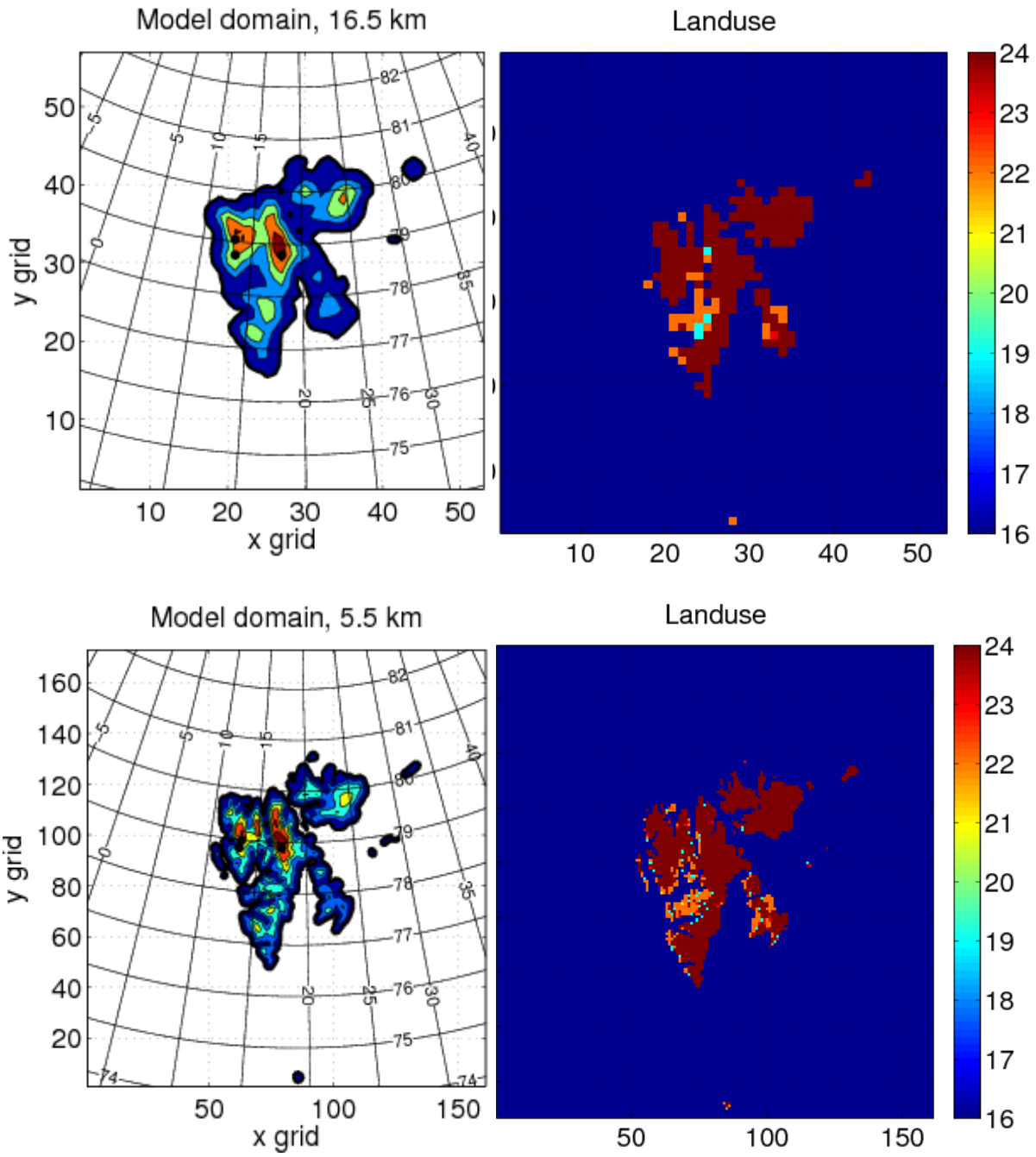

Figure 1. (left)The model domain, with the investigated sites marked by dots. Kongsvegen and Holtedalfonna (north of Kongsvegen) are situated in the north-western Spitsbergen and Lomonosovfinna in the north-eastern Spitsbergen. Contour lines show elevation with 200 m equidistance. (right) NPI land use map, with dark red being glacier, turquoise barren or sparsely vegetated tundra, orange mixed tundra and blue water. The upper(lower) panels correspond to a model resolution of 16.5 km (5.5 km).

The WRF model (Skamarock et al. 2008) is an open source atmospheric model (http://www.mmm.ucar.edu/wrf/users/) widely used in research as well as other applications

and can be run at horizontal resolutions ranging from 100 kilometres down to sub-km scale. The model simulations conducted in this investigation had a horizontal resolution of 16.5 km (or 5.5 km in a resolution sensitivity test) and the model set-up was basically that of the study by Claremar et al. (2012) but for the WRF3.6 version. In Claremar et al. (2012) various physics schemes were changed in a sensitivity study. Here we use the Morrison double-moment microphysics scheme (Morrison et al. 2005) and the MYNN2.5 turbulence scheme (Nakanishi and Niino 2006). The land surface scheme is alternated between the CLM4 land surface scheme (Lawrence et al. 2011) with the sophisticated SNICAR albedo scheme (Flanner & Zender 2005; Flanner et al. 2007) and NoahMP (Niu et al. 2011) with the simpler BATS scheme (Yang et al. 1997). Forcing data were from the ERA-Interim re-analysis (Dee et al. 2011). The sea surface temperature (SST) is taken from OSTIA (Donlon et al. 2012) where the resolution is as fine as 0.05° (i.e. 5.5 km in N-S direction and about 1 km in W-E). Terrain and land use data are originally from USGS (U.S. Geological Survey) but here the land use/glacier mask is taken from NPI (Nuth et al. 2013). Fig. 1 shows the model grid, terrain and landuse mask.

Snow schemes

In the WRF model several different land surface models/schemes (LSMs) can be used. In a previous report (Claremar 2013) the Noah-MP scheme (Niu et al. 2011, Yang and Niu 2003) was used. It has 3 snow layers and liquid water retention and refreezing already implemented. Snow compaction is accounted for following Anderson (1976) and Sun et al. (1999). Claremar (2013) showed that 3 layers gave too coarse resolution in the thermal and hydrological development in the snow. Depending on the snow depth the snow consists of one to three layers. The uppermost layer is limited to 5 cm, the middle one to 20 cm (adding up to 25 cm) and the lowest is limited by the snow depth which in turn is limited by a maximum of 2 mwe snow water equivalent (SWE) and thus can be several meters thick, depending on the density. This thick layer limits the possibility to describe the snow evolution and work with the introduction of more layers was started but has not been completed, as the architecture of the program code delimited the possibility to do so in the available time frame. However, the soil layers in the Noah-MP scheme use firn/glacier properties. The firn layer thicknesses are constant, being 0.1, 0.3, 0.6 and 1 m, counting from above, which adds up to 2 m. Densities are not explicitly calculated but thermal conductivity and capacity are functions of depth. Liquid water and refreezing is accounted for and can be tracked but the water holding capacity is unlimited. Snow albedo parameterization is from the BATS scheme (Yang et al., 1997) and is further presented in the next sub-section. Division of precipitation into snowfall and rain is done following the relatively complex functional form of Jordan (1991). The CLM4 scheme (Lawrence et al. 2011) has up to 5 snow layers and a more sophisticated albedo scheme (SNICAR). The layer thicknesses for deep snow are, counting from surface, 2, 5, 11, 23 cm (thus adding up to 41 cm) and for the deepest layer about 100 cm, depending on the density and SWE (maximum 1 mwe).

Albedo schemes

SNICAR

The snow albedo and snow layer absorption in the SNICAR (SNow, ICe and Aerosol Radiative model) scheme (Flanner & Zender 2005; Flanner et al. 2007) uses two-stream radiative transfer (Toon et al. 1989). That means that the radiation balance is calculated for each snow layer with both down- and upwelling components. The profiles of albedo and absorption are functions of solar zenith angle, albedo of the underlying snow, mass concentration of atmospheric-deposited aerosols and effective snow grain size. The latter is simulated by a snow aging routine. The grain shape is assumed to be spheres. Each layer uses

the optical properties: single-scattering albedo ω, extinction optical depth (m^2 kg^{-1}), τ, and asymmetry parameter, g, all in 5 different spectral bands (separated and limited at 0.3µm,0.7 µm, 1µm, 1.2µm, 1.5µm and 5µm) and for different snow grain sizes and aerosol species. A subset of values can be found in look-up tables 3.5 to 3.7 in Oleson et al. (2010). These parameters valid for the snow as function of spectral bands and radii between 30 an 1500µm and with 1µm resolution are read as input files to the WRF model.

Here we evaluate the sensitivity of snow albedo to the assumed snow grain shape by testing in SNICAR the Optimized Habit Combination grain shapes, *OHC* of Räisänen et al. (2015). This is a combination of severely rough droxtals, aggregates of severely rough plates and strongly distorted Koch fractals. The main difference to spheres is that for the OHC, the asymmetry parameter g is lower, and consequently, for a given snow water equivalent and snow grain size, snow albedo is higher, especially for the IR part of the spectrum.

BATS

The BATS scheme is divided into two spectral bands, visible (VIS) and infrared (IR), separated at 0.7µm, and further into direct and diffuse albedo (Yang et al. 1997). A snow age factor accounts for the darkening of the snow after snowfall. By default this factor is set to zero for glacier snow, giving albedo only dependent on solar elevation. In the current simulations the glacier snow aging is activated.

The total albedo is given divided equally into VIS and IR parts:

$$A = 0.5(A_V + A_{IR})$$

where the visible and IR parts are given by:

$$A_V = A_{V,D} + 0.4 f_z (1 - A_{V,D})$$
$$A_{IR} = A_{IR,D} + 0.4 f_z (1 - A_{IR,D})$$

The factor f_z describes the enhancement of the direct (black-sky) albedo at large solar zenith angles and is expressed as:

$$f_z = \max\left[0, \frac{1}{b}\left(\frac{1+b}{1+2b\cos Z} - 1\right)\right]$$

where Z is the solar zenith angle and b = 2 in BATS. With solar elevation higher than 30° (Z<60°) f_z =0, which means that the albedo for direct solar radiation is assumed to be the same as for diffuse radiation.

The diffuse components are given by

$$A_{V,D} = A_{V,0}(1 - 0.2 f_{age})$$
$$A_{IR,D} = A_{IR,0}(1 - 0.5 f_{age})$$

where the snow age factor is dependent on time since last snowfall, the amount of current snow fall (a liquid-water equivalent of 10 mm is required to restore the maximum albedo), grain growth due to water vapour diffusion and close to melt point, both affected by snow surface temperature, and also a constant effect of dirt and soot. Colder snow delays the aging. The maximum new snow albedos, given by index 0 is by default 0.95 for the visible band and 0.65 for the IR short wave radiation. For details, see Yang et al. (1997).

For sensitivity tests, the new snow spectral band albedos in SNICAR, calculated for 55µm snow grains (the new snow radius in SNICAR) were averaged over the VIS and IR bands and inserted into BATS. The resulting albedos (index 0) were then 0.99 for VIS for both spheres and the OHC and for IR 0.73 for spheres and 0.76 for the OHC, respectively. All these are thus higher than in the original BATS scheme.

MEASUREMENTS

Albedo measurements both from in-situ observations and MODIS satellite images are considered. The in-situ observations are from three sites on the glaciers Lomonosovfonna, Kongsvegen and Holtedalfonna (Fig. 1). The automatic weather station (AWS) at Nordenskiöldbreen is used to find the best validation point for Lomonosovfonna. All data used are from the summer season of 2013.

AWS stations

For validation of the 2-m temperature simulated by the model we use measurements from an AWS at Nordenskiöldbreen (78°41'39"N, 17°09'22"E, 530 m a.s.l.). The AWS is situated in the central flow line of the glacier, which is confined by steep slopes to the north and to the south.

The Lomonosovfonna AWS (LF) is situated at 78°50"N, 17°26"E and 1200 m a.s.l. and placed on the dome of this ice field. In addition to radiation we also use temperature data from this station. Kongsvegen upper AWS (KNG6), lies at 78°47"N, 13°9"E and 534 m. The Holtedalfonna AWS (HDF4.5) is placed at 78°59', 13°37' and 684 m. Radiation is measured by a Kipp & Zonen CNR1 radiometer on all sites.

MODIS

For spatial validation MODerate resolution Imaging Spectroradiometer (MODIS) output at 500 m resolution was used. Two products were deployed. The 1-day albedo from MOD10A1 from the Terra satellite (Hall et al. 2006) and the 16-day albedo from MCD43A3, a combination of data from the Aqua and Terra satellites. In the latter product daily values are weighted and averaged as a function of quality, observation coverage and temporal distance from the day of interest. In Stroeve et al. (2013) these data are evaluated against AWSs on Greenland, with rather good results, although with some errors.

METHODOLOGY

In comparing the modelled albedos with in-situ observations, an attempt is made to account for the WRF model's temperature bias. To evaluate the temperature bias, we use temperature measurements from Nordensköldbreen as reference. On average, the WRF features a cold bias of about –1.8 °C in the Sep to June period when the cold content in the snow is determined. The surface temperature lapse rate of the model in the same period is about 5.5°C/km. Since there is a cold bias we can find the correct temperature about 300 m further down. Thus, assuming that the simulated lapse rates are correct, a point was chosen with height 910 m close to Lomonosovfonna (1200 m a.s.l.) and along the north-south ridge (to minimize west/east barrier effects on precipitation). The temperatures from KNG and HDF were not available in the time frame of this report.

The MODIS data can be used both for point and spatial evaluation of the WRF albedo. An issue is how to interpret the MODIS vs. in-situ data which show substantial deviations from each other. The 16-day (MCD43A1) and 1-day MODIS (MOD10A1), both at 500 m, were compared with in-situ observations to determine which product should be used. Both the MODIS pixel closest to the in-situ sites and an average of 9 pixels around the station, i.e. a 1.5 km grid, were used. The latter was used to estimate some uncertainties related to high-angle contribution to the upwelling SW radiation. To only include snow-covered pixels in the comparison, albedo values less than 0.6 were omitted and in the 1-day albedo product also at least 95 % snow covered grid and good quality flags were required. No filtering of the 16-day albedo other than the in-built functions was performed. The results are given in Fig. 2. It is

seen that the 16-day albedo is substantially lower than the 1-day albedo. The 1-day albedo is closer to the in-situ observations (Fig. 2) but it can jump up and down from day to day by up to 0.25 albedo units. The 1 and 9 pixels grid do not differ considerably, which indicate a rather homogeneous surface, as seen by the satellite.

Because of the bias in the 16-day albedo we use the 1-day albedo in the comparison to the WRF model. In the following comparisons the MODIS albedo is both presented as 1.5 km grid (referred to as point) and the WRF grid (16.5 km), using the 75th percentile of 121 points surrounding the WRF grid centre to be sure to evaluate snow). The former should represent the in-situ measurements and the latter the WRF output, assuming that the WRF grid consists of 100 % snow.

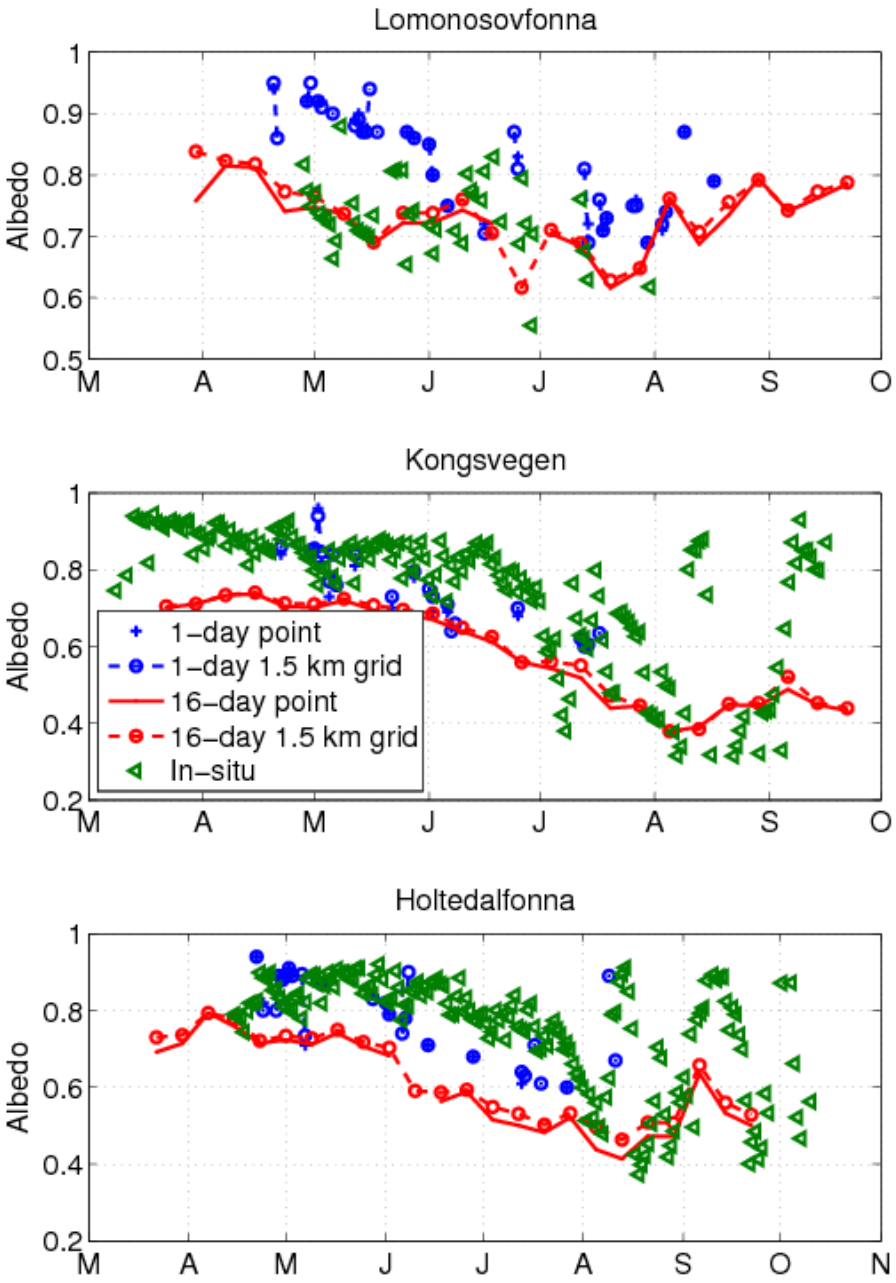

Fig. 2. Observations of albedo with MODIS and in-situ data at three glacier sites. MODIS albedo is represented by both in-situ (1 grid point) and the average within a 1.5 km grid surrounding the site.

SIMULATIONS

Several sensitivity type simulations were conducted with the WRF model, as summarized in Table 1. The change of albedo due to snow grain structure was investigated both using the CLM4 (SNICAR) and NoahMP (BATS) snow schemes. The albedos in BATS were originally rather low compared to what is used in SNICAR. We hence also investigate the effect of increasing it to the ones simulated by SNICAR. Also the effect from aging is investigated by comparing the experiment Ref2013_95_85 with Ref2013_95_85_fage2, where the aging effect f_{age} is doubled. Here we force the new snow albedo to about 0.90 (95 for VIS and 85 for IR). In general the Noah-MP scheme makes the simulations run about five times faster. Further the runs with CLM4 are numerically more unstable.

Table 1. The simulations performed.

Run	Surface/ snow scheme	Albedo
Ref	CLM/SNICAR	Original sphere tables
OHC	CLM/SNICAR	OHC albedo tables
Ref	Noah-MP/BATS	Original BATS scheme
Ref2013_95_85	Noah-MP/BATS	95% for VIS and 85 % for IR
Ref2013_95_85_fage2	Noah-MP/BATS	As above but with double aging speed
Sph2013_99_73	Noah-MP/BATS	With sphere values for VIS and IR from SNICAR. 99% albedo for VIS and 73% for IR.
OHC2013_99_76	Noah-MP/BATS	With OHC values for VIS and IR. 99% albedo for VIS and 76 % for IR
OHC2013_99_76_5km	Noah-MP/BATS	Same as above but with 5.5 km resolution.

The WRF simulations start on 31 Jan 2013 for the CLM4 simulations and on 1 April 2013 for NoahMP and are run until the middle of August. The rather late starts were motivated by the computer resources and the fact that focus was on the surface of the snow. The start for CLM4 in the winter was motivated by that the snow is reset to zero at start. Still it was noted that not sufficient snow was created during the simulation so total melt occurs too early in the CLM4 simulations. For Noah-MP 1 April is sufficient for the snow depth since the snow depth is not reset at start. However, this late start for Noah-MP means that the deep snow may be colder or warmer, compared to if a whole winter cycle is simulated. An effect of this is a too early surface melt or a delay of surface melt and hence a mistiming of the fast albedo drop. Therefore the focus in the comparisons is for the first part of the summer, i.e. ending in the end of June or in July, depending on site.

For comparison, models grid point are chosen as close to the AWS sites as possible. For LF the position is 78°47'52"N, 17°58'24"E and 911 m (1200 m), for KNG 78°44'45"N, 13°23'29"E and 622 m (534 m) and for HDF 79°2'32"N, 13°14'18"E and 745 (684 m), where

the elevation of the AWS sites is given in parentheses. We know that for LF the 2-m temperature is well simulated at the elevation 300 m below the station because of a general negative bias. One can then expect that T2 is underestimated at KNG and HF and thus the albedo overestimated, at least later on in the summer.

RESULTS

CLM4/SNICAR

We analyze here the effect of changed grain structure assumptions on albedos simulated by the WRF model. For comparison the in-situ measurements and MODIS 1-day data are used. This is to capture the variability in the MODIS measurements as well.

In Figure 2a the albedo from Lomonosovfonna is shown. It is evident that use of non-spherical snow grains (OHC) enhances the albedo but only moderately, about 0.03 units. Comparing with observations it is evident that the variability is not captured with the SNICAR model. This should not however be expected in the end of the season because the timing of melt may not be captured. The WRF albedo levels are in better agreement with the MODIS observations but still the variability is less in WRF. It is interesting to note however that the in-situ and MODIS observations disagree considerably at Lomonosovfonna. It is very difficult to evaluate if the OHC or sphere grain shapes performs the best here. At Kongsvegen and Holtedalfonna (Fig. 2b, c) the agreement is much better, both to in-situ and MODIS albedo. At these sites OHC performed better most of the time compared to the in-situ measurements. Short-term variability is still somewhat underestimated, especially if looking at MODIS daily data. The long-term decrease of albedo is well captured by the model at these sites. The timing of snowfall events is not sufficiently reproduced but may be improved with higher horizontal resolution. The results here suggest that the MODIS albedo rather well describes the real albedo but that the in-situ observations at Lomonosovfonna may have some problems. We therefore rely on the MODIS 1-day albedo in the comparisons.

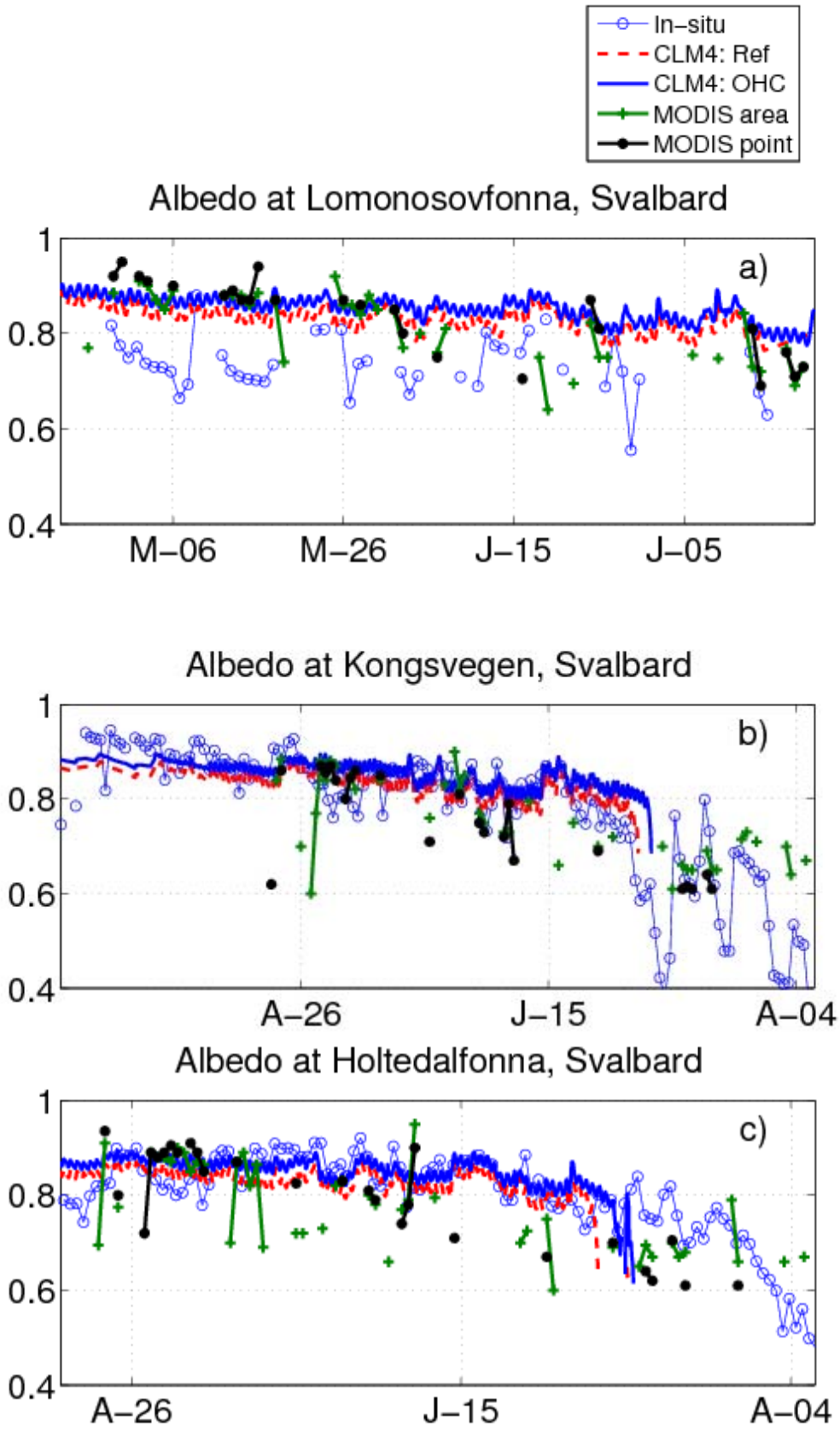

Fig. 3. Observed and simulated SNICAR albedo with different snow grain shapes at the three sites. MODIS data are 1-day. MODIS area represent 75th percentile in a 5 x 5 km square surrounding the WRF grid point.

From these figures one cannot tell if OHC outperforms the spherical grains. Comparing with spatially averaged MODIS 1-day (not shown) suggests underestimation for all simulations. The spatial averages of the albedo difference to MODIS 16-day data for all snow points (90th percentile) are shown in Fig. 4. It is seen that the simulation with spheres better represents the snow albedo throughout the period. This finding should be interpreted with caution, since the albedo biases can be influenced by errors in other factors than snow grain shape, such as the simulated snow grain size and impurity concentration. In addition, as noted above, the MODIS 1-day albedos are higher than the 16-day albedo. However, the rather constant deviation by the SNICAR scheme points at good long-term aging.

Shown also is the albedo from the original Noah-MP/BATS scheme, which is, on average, a clear underestimate. However, in the later part of the season (before extensive melting) the albedo approaches the MODIS observations, an indication that the aging effect is too small.

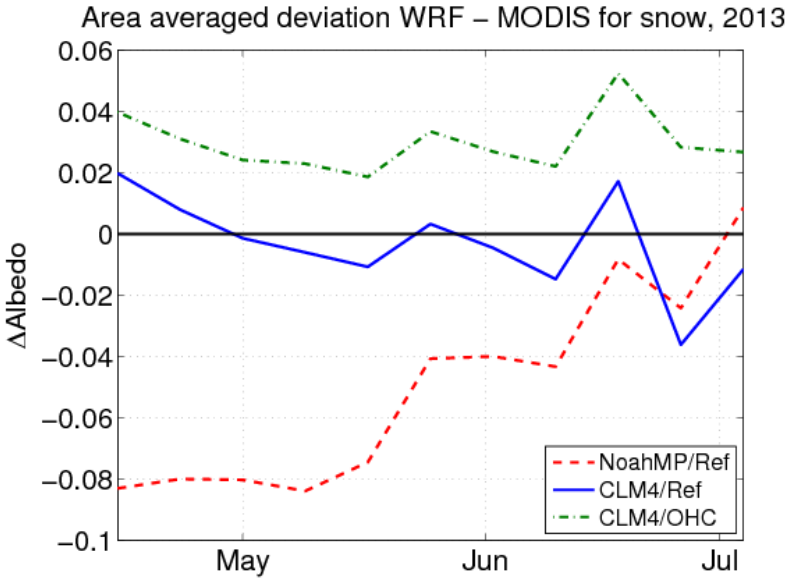

Figure 4. Deviation of WRF albedo to 16-day MODIS.

Simulated 2-m temperature (T2) at LF is show in Fig. 5. It is seen that outliers vanish with OHC because of later melt of the too thin snow. In Table 2 it can be noted that the T2 is lowered by 0.35K on average with the OHC. Thus a negative bias gets even more negative. It is mainly the positive temperatures that are underestimated. It should be recalled that the model grid point used for comparison is located lower (910 m) than the LF AWS (1200 m). Therefore, the values in Table 2 and Fig. 5 do not represent the absolute values of the temperature bias (which are on average nearly 2K more negative) but rather values relevant for the albedo comparison.

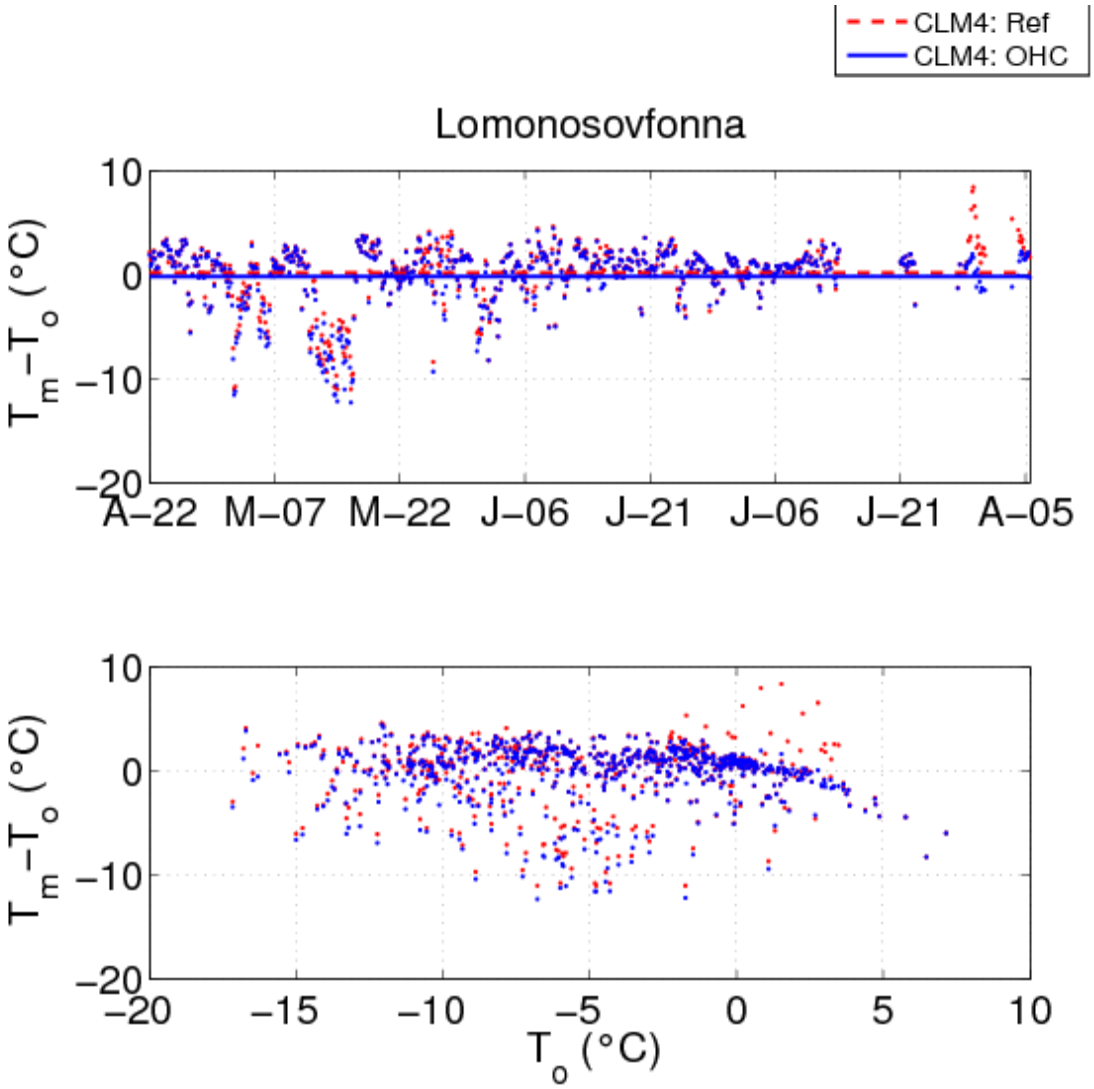

Figure 5. Simulated (SNICAR) 2-m temperature (T_m) compared to observed (T_o)

Table 2. Temperature bias at Lomonosovfonna (LF) for the CLM4 simulations.

	Bias 22 April to 20 Aug	Bias 22 April to 31 May
Ref	0.15	-0.59
OHC	-0.21	-0.96

The small average T2 biases secures the turbulent heat flux to the snow, given a correct skin temperature (which, however, indeed is very dependent on a correct radiation balance). The effect of changed albedo on snow temperature at LF is shown in Fig. 6. Ideally the snow thickness should be about 2 m in the model but since it is less than 1 m it is able to melt around the July to August transition. The use of OHC shapes of course dampens the heating and melt. The change in snow melt is quite substantial considering that the albedo only differs by a couple of percent.

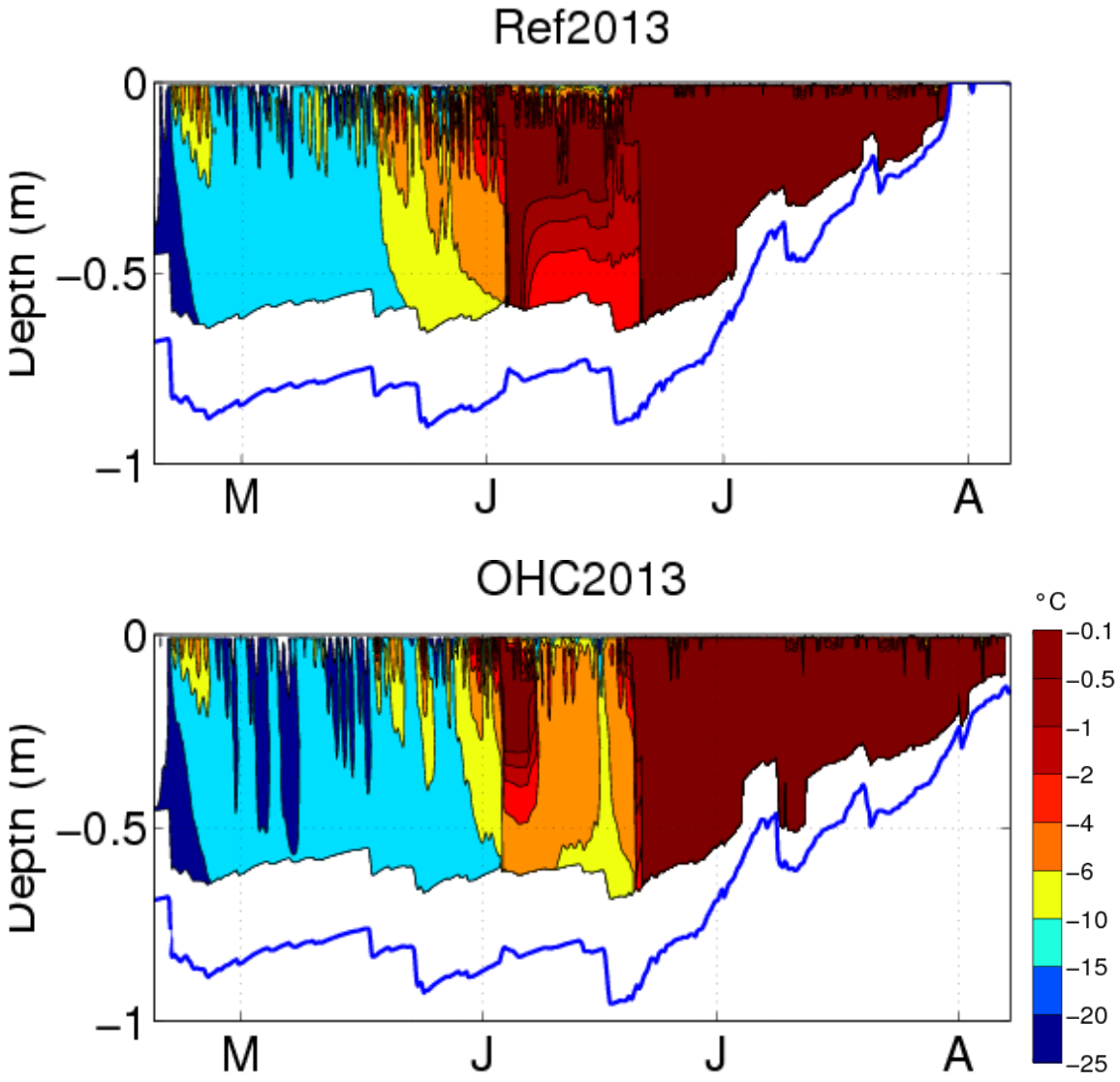

Figure 6. Simulated (CLM4) snow temperature at snow layer centre depths and snow depth (blue line).

Noah-MP/BATS

The simulations with the Noah-MP surface scheme are presented here. The differences between reference settings and the albedo parameter values for new snow taken for spheres and OHC shapes, respectively, from SNICAR are shown in Fig. 7. Note that the reference run has a spin-up from 28 Aug the year before giving more representative snow temperatures and depth. Thus the comparison should be focused on the period May to beginning or end of July depending on site. At LF the simulated albedo is close to the in-situ observations on average but lower than the MODIS 1-day albedo. At the other sites the albedos are too low in the beginning of the season and similar to MODIS 1-day and in-situ albedos from July (KNG) or August (HDF) and higher than the in-situ observations. The use of SNICAR albedos for new snow increases the albedo but starting from May, the change is moderate at KNG and HDF if one compares with the CLM4 runs. Furthermore, even when the albedo for new snow is based on SNICAR, Noah-MP produces albedos lower than in SNICAR, from 0.85–0.90 in CLM4 to seldom above 0.8 in Noah-MP. This must be an effect of the aging parameter in Noah-MP.

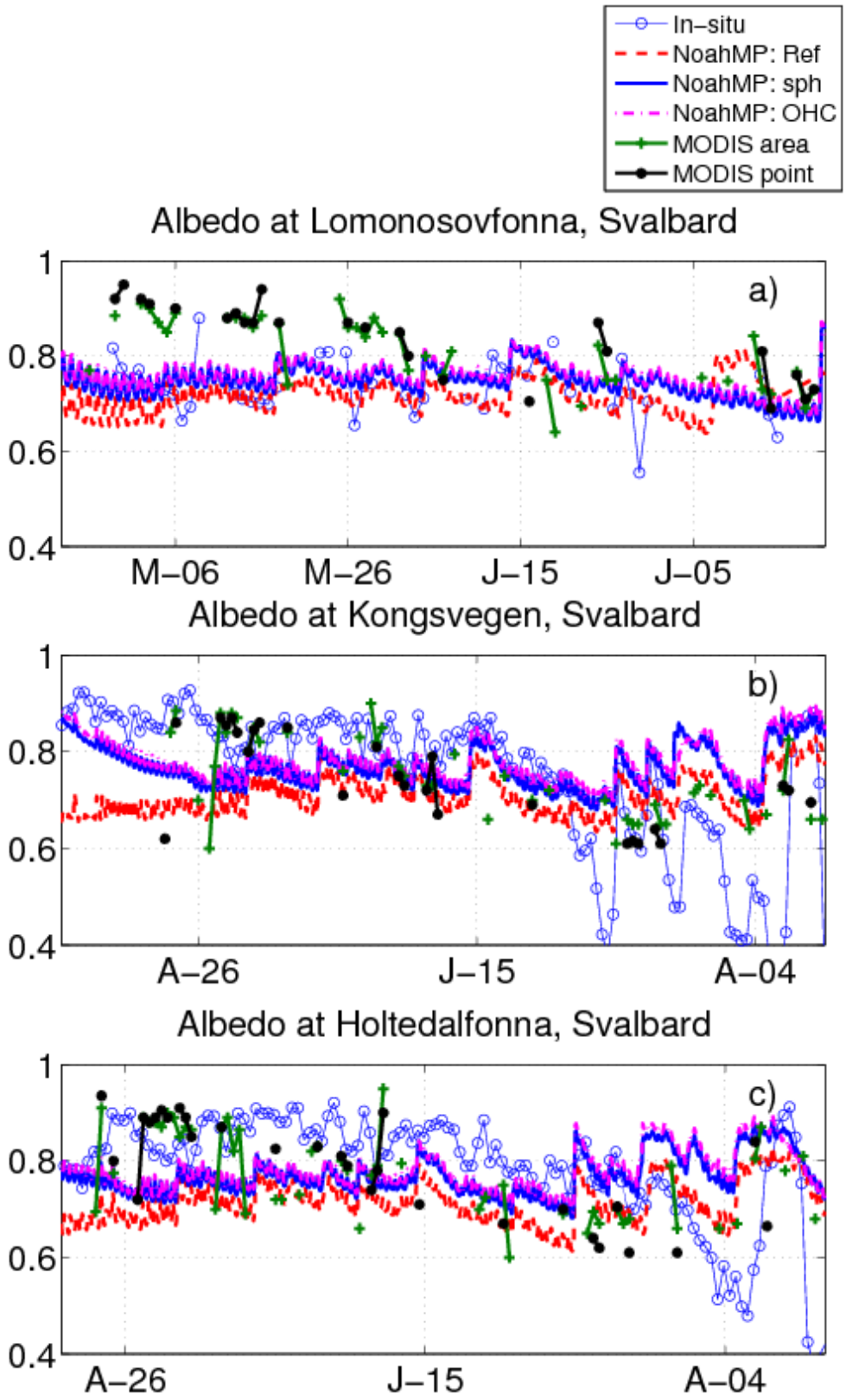

Fig. 7. Observed and simulated BATS albedo with original BATS and different snow grain shapes at the three sites. MODIS data are from the 1-day product. "MODIS area" represents the 75th percentile in a 5 x 5 km square surrounding the WRF grid point.

The temporal variability of albedo is not very well simulated. Therefore we analyse the sensitivity to doubling the aging parameter, f_{age}. The start value of the albedo for new snow is

about 0.9 (0.95 for VIS and 0.85 for IR) and is hence slightly higher than in the Noah-MP_OHC simulations. The albedo is shown in Fig 8. With doubled aging effect the mean albedo is close to the BATS reference simulations although at large snow falls the albedo rises to 0.9. The timing of the snowfall events also makes it difficult at this stage to find a proper expression. The variability is however better simulated although the aging is too fast and the long seasonal darkening is not captured. This suggests that one should change the subparts of the aging parameter, rather than just double it. Overall, we would like to get higher albedo values while also capturing the temporal variability.

To see if the timing of snowfall and the albedo variations is improved by better horizontal resolution, WRF 5 km was compared to 16 km, using the OHC albedo. In Fig. 9 one can see that the effects are minor. The most significant change is however the timing of some snowfall. Whether it is better with the 5 km resolution is not evident though.

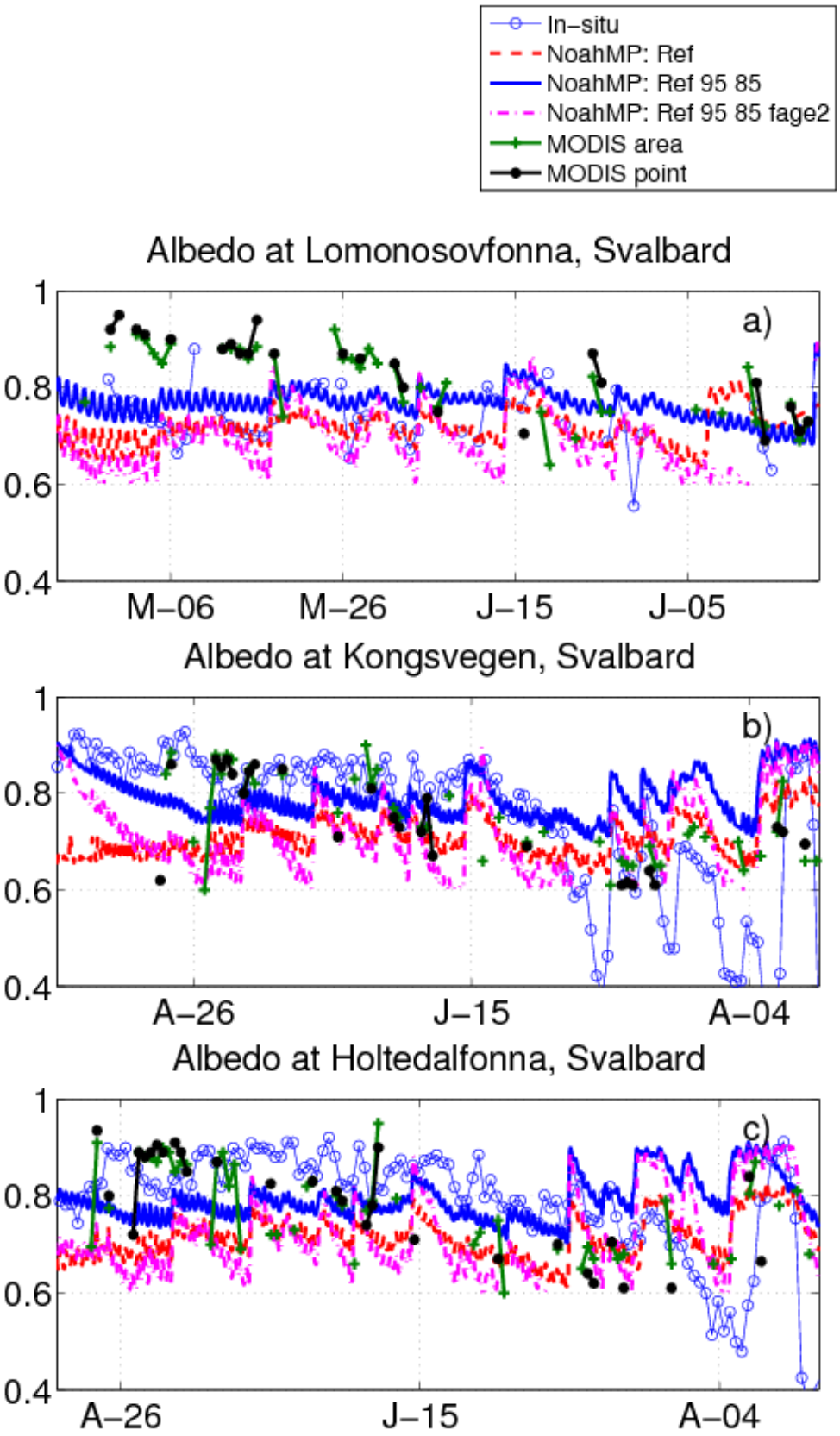

Fig. 8. Observed and simulated BATS albedo with original BATS and different aging parameters at the three sites. MODIS data are from the 1-day product. "MODIS area" represent the 75th percentile in a 5 x 5 km square surrounding the WRF grid point.

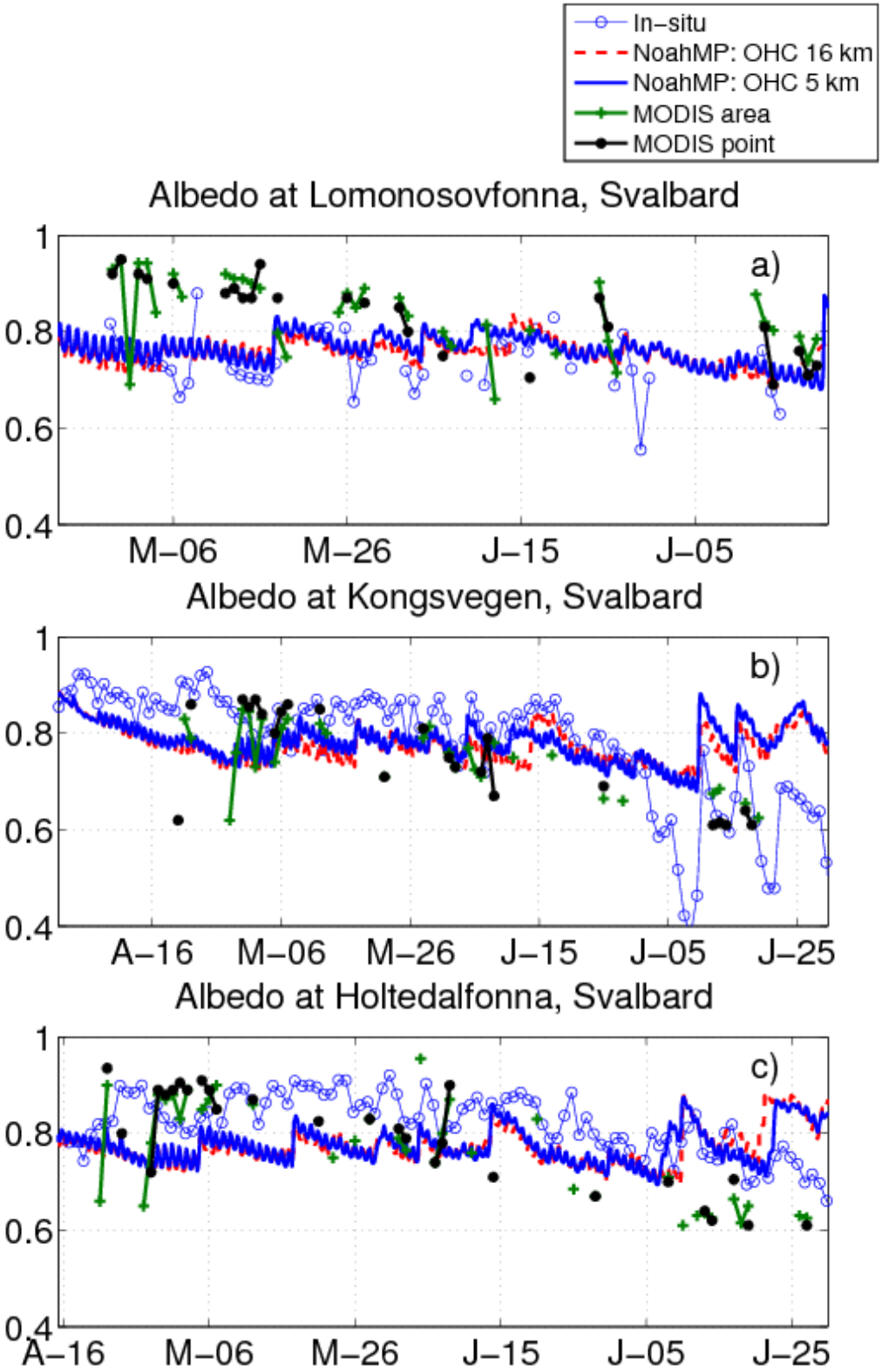

Fig. 9. Observed and simulated BATS albedo with OHC grain shapes and different resolutions at the three sites. MODIS data are from the 1-day product. "MODIS area" represent the 75th percentile in a 5 x 5 km square surrounding the WRF grid point.

Simulated 2-m temperature (T2) at LF with Noah-MP are on average less sensitive to albedo changes than for CLM4. In Table 3 it can be noted that the bias is mostly positive but close to zero, having in mind that the WRF grid is 300 m further down, (about 2°C topographically adjusted negative bias). T2 is lowered the most by introducing the SNICAR new snow values for the OHC shape. Thus a negative adjusted bias gets even more negative. As for CLM4 it is mainly the positive temperatures that are underestimated. The transition from spheres to OHC grains has a lesser effect than for CLM4, probably because of the aging effect that decreases the relative difference in absorption (1-albedo). Doubling the aging parameter increases the temperature by 0.35°C for the complete period and 0.5°C in April–May giving even higher T2 than the reference.

Table 3. Temperature bias at Lomonosovfonna (LF) for the Noah-MP simulations.

	Bias 22 April to 20 Aug	Bias 22 April to 31 May
Ref	0.27	0.19
Sph2013_99_73	0.20	0.01
OHC2013_99_76	0.16	-0.06
Ref2013_95_85	0.10	-0.13
Ref2013_95_85_fage2	0.45	0.39

Also here the T2 is a good forcer to the snow temperature, given a correct radiation balance. The effect of different albedos on snow temperature in Noah-MP is less than in the CLM4 simulations, mainly due to the deeper snow in Noah-MP. Comparing with CLM4 the snow is heated much slower in Noah-MP, even though the initial snow temperature close to the surface is much higher in Noah-MP. This is probably due to the fact that the short wave radiation is absorbed only in the uppermost layer, or actually at the surface. The heat is then conducted through the snow. But the main melt events in the beginning of June and around 20th June are seen in both Noah-MP and CLM4. In Noah-MP water percolates through the snow in the beginning of July but this happens already on 20 June in Noah-CLM4. Note that the lower boundary conditions are different in the two snow schemes. The effect of grain shape is shown as well in Fig. 10 but the difference is minor compared to the CLM4 simulations.

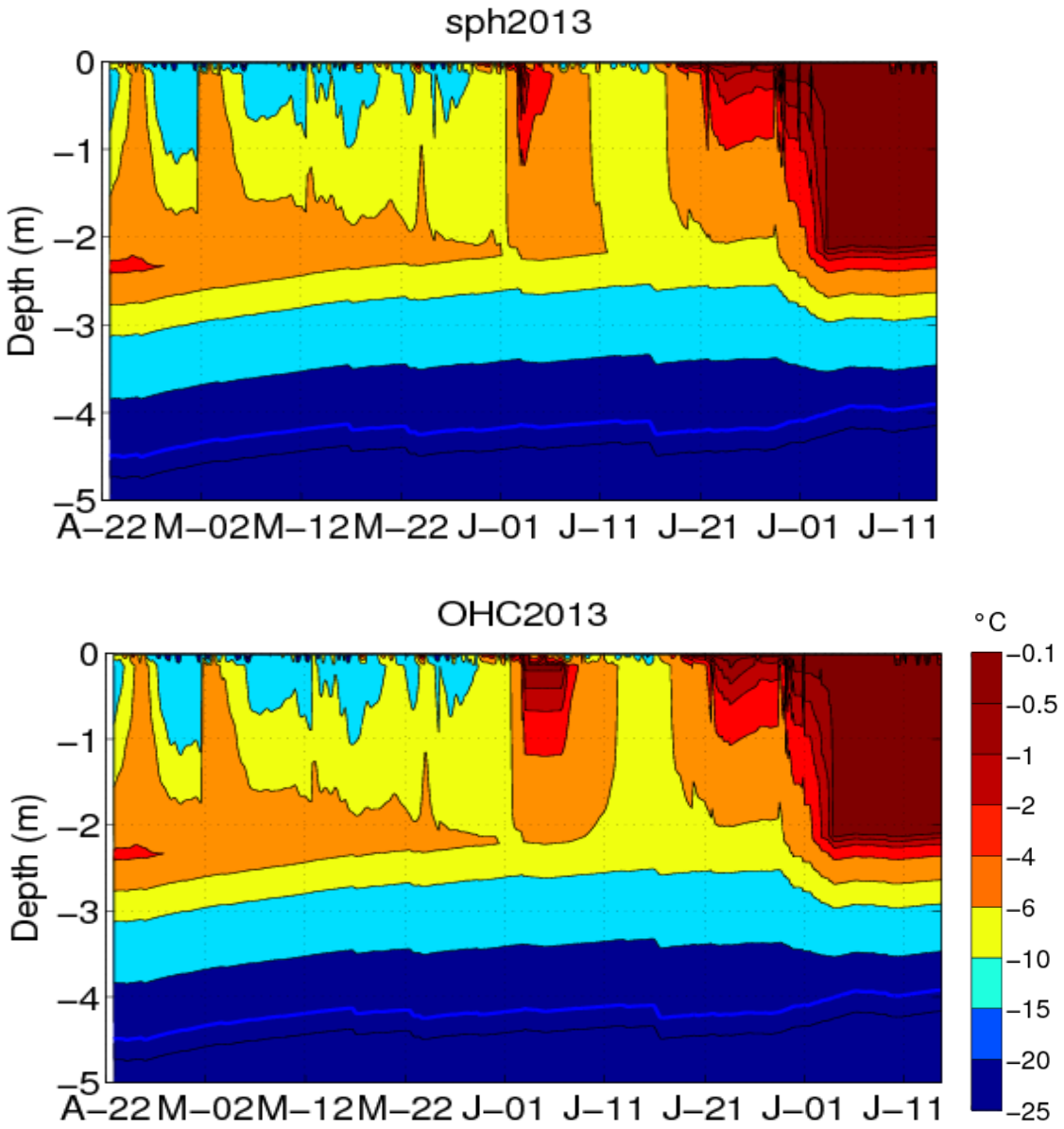

Figure 10. Simulated (Noah-MP) snow temperature at snow layer centre depths and snow depth (blue line).

DISCUSSION AND CONCLUSIONS

This study was initiated to investigate the snow albedo over glaciers at Svalbard as simulated in the WRF model in two different snow schemes. For regional climate simulations on the order of 20 years with 5 km horizontal resolution it is not practicable to use the CLM4 land surface scheme with SNICAR because of the computer resources needed. But for short-period studies it can be interesting. Since it includes two-way radiative transfer and penetration into the snow it is expected that it performs well. In this scheme snow single-scattering parameters like extinction coefficient, single-scattering albedo and asymmetry parameter could be directly inserted. We tested the effect on albedo calculations due to the use of parameters based on the Optimized Habit Combination (OHC) snow grain shapes (Räisänen et al. 2015). These should be more representative than spheres only. Also the performance of the snow scheme BATS (in NoahMP) and the effect of changing some tuning

parameters was studied in order to find out good values for climate simulations over the Svalbard region.

Because of the short initialisation of the snow pack in the simulations there was no expectation that the snow temperature deeper in the snowpack is correct but rather the sensitivity was studied. The albedo in WRF was directly compared to in-situ measurements at three glaciers as well as remote sensing MODIS satellite albedo. The MODIS and in-situ observations gave similar (but not identical) results except for the Lomonosovfonna in-situ observations. Omitting those measurements the albedo is over-estimated by the SNICAR scheme but underestimated by the original BATS scheme. The albedo products from MODIS, 1-day and 16 -days were very different from each-other, with filtered 1-day values higher than the 16-day product. The 16-day product was closer to the in-situ observations at Lomonosovfonna but the 1-day albedo was closer at Kongsvegen and Holtedalfonna, where also the SNICAR albedo was close to the observations. However the spatially averaged MODIS 16-day albedo was closer to the SNICAR simulations. This discrepancy between the MODIS product requires further investigation.

Due to the observational uncertainties, it could not be sorted out which grain shape should be used. Both grain shapes were used to modify the new snow albedo in the BATS scheme. OHC gives the highest albedo, just above the spheres, but well above the original BATS albedo. Because of a different aging routine the albedo is still lower than in SNICAR. This suggests a slower aging but the high-frequency changes in the observations point to a need for modifying the sub-parts of the aging routine, keeping both high- and low-frequency fluctuations in the albedo, for instance changing grain growth parameter and dust separately. The grain growth acts on a short time scale and may be the reason why SNICAR underestimates the short-term variability. 5.5 km resolution does not significantly improve the comparison with the site albedos, but should preferably be used since the local terrain effects on precipitation are better simulated.

The effect on T2 and the snow temperature was investigated at Lomonosovfonna. T2 is negatively biased by about 2°C in the reference simulations and increasing the albedo has a further cooling effect by a few tens of a degree. Therefore it is more probable that the bias is mainly due to other factors like too little cloud cover and unlimited cooling during clear and very stable nights because of cut-off of the simulated turbulent fluxes. The snow temperatures in CLM4 and Noah-MP behave differently due to the absorption in the snow in CLM4. Therefore the snow is heated faster in the upper 10s of cm compared to in Noah-MP. In Claremar (2015) it was shown that a higher snow thermal conductivity than reported in laboratory or field was needed to simulate a correct snow temperature in Noah-MP. This is probably due to the lack of heating by deep absorption of the snow.

In future studies, albedo and snow products from the MODIS satellite instrument should be investigated further to understand why they differ. MODIS images may also be utilized to find snow lines and compare to WRF simulations. Further, the surface energy balance at the sites should be investigated to sort out if the incoming shortwave radiation is of larger importance than the albedo.

To conclude:

- Different MODIS products are not in agreement with in-situ measurements
- In CLM4 the surface snow is heated by penetrating short wave radiation that is absorbed by the snow. This is probably why the summer snow temperature is much higher in CLM4 and why Noah-MP requires a high snow thermal conductivity.
- The effect of grain shape on albedo is small but significant on T2 and snow temperature.

- It is not evident if spherical snow grains or the OHC perform better.
- Further work is required to capture the aging effect on the albedo.

Acknowledgements

Sergey Marchenko and Veijo Pohjola at Uppsala University and Carl Egede Bøggild at DTU are thanked for input and discussions. Thanks to Kjetil Schanke Aas I could get use of the OSTIA data provided by MYOCEAN and the glacial mask from NPI. Carleen Reijmer at University of Utrecht provided the AWS data from Nordenskiöldbreen and Ward van Pelt/ Jag Kohler provided the AWS data from Kongsvegen and Holtedalfonna. Simulations were performed at UPPMAX, Uppsala University. The work was funded by the Nordic council of ministers (SVALI, www.ncoe-svali.org) and in part by the Academy of Finland through the A4 project (grant number 254195)

References

Anderson, E.A. (1976). A point energy mass balance model of a snow cover. NOAA Tech. Rep. NWS 19, 150 pp., Off. of Hydrol., Natl. Weather Serv., Silver Springs, Md.

Claremar, B., Obleitner, F., Reijmer, C., Pohjola, V., Waxegård, A. et al. (2012). Applying a Mesoscale Atmospheric Model to Svalbard Glaciers. Advances in Meteorology. 321649

Claremar, B 2013. Water retention parameterization in the WRF model — A sensitivity test. SVALI report D3.1-1.

Claremar, B 2015. Glacier snow sub-surface properties on Svalbard in the atmospheric model WRF. SVALI report D3.1-5.

Dee, D. P., Uppala, S. M., Simmons, A. J., Berrisford, P., Poli, P., et al. (2011). The ERA-Interim reanalysis: configuration and performance of the data assimilation system. Q.J.R. Meteorol. Soc., 137: 553–597. doi: 10.1002/qj.828

Donlon et al. 2012, The Operational Sea Surface Temperature and Sea Ice Analysis (OSTIA) system. Remote Sens. Environ., 116, 140–158.

Hall, D. K., V. V. Salomonson, and G. A. Riggs. 2006. *MODIS/Terra Snow Cover Daily L3 Global 500m Grid.* Version 5. [indicate subset used]. Boulder, Colorado USA: NASA National Snow and Ice Data Center Distributed Active Archive Center.

Jordan 1991. A one-dimensional temperature model for a snow cover. CRREL SP 91-16.

Lawrence et al. 2011. Parameterization Improvements and Functional and Structural Advances in Version 4 of the Community Land Model. J. Adv. Model. Earth Sys., 3, DOI: 10.1029/2011MS00004.

H. Morrison, J. A. Curry, and V. I. Khvorostyanov (2005), A new double-moment microphysics parameterization for application in cloud and climate models. Part I: Description. J. Atm. Sci., vol. 62, no. 6, 1665–1677.

Nakanishi, M. and Niino H. (2006), An Improved Mellor–Yamada Level-3 Model: Its Numerical Stability and Application to a Regional Prediction of Advection Fog, Boundary-Layer Meteorol., vol. 119, no. 2, pp. 397–407.

Niu, G.-Y., Yang Z.-L., Mitchell K.E., Chen F., Ek, M.B., et al 2011. The community Noah land surface model with multiparameterization options (Noah-MP): 1. Model description and evaluation with local-scale measurements. J. Geophys. Res., 116, D12109, doi: 10.1029/2010JD015139.

Nuth et al. 2013. Decadal changes from a multi-temporal glacier inventory of Svalbard. The Cryosphere Discuss., 7, 1603–1621.

Oleson et al. 2010. Technical Description of version 4.0 of the Community Land Model (CLM)

Räisänen, P., Kokhanovsky, A., Guyot, G., Jourdan, O., and Nousiainen, T., 2015. Parameterization of single-scattering properties of snow, The Cryosphere, 9, 1277-1301, doi:10.5194/tc-9-1277-2015, 2015.

Schneider, T. and Jansson, P 2004. Internal accumulation in firn and its significance for the mass balance of Storglaciären, Sweden. J. Glaciol., 50, 25–34.

Skamarock, W. C. et al. 2008, "A description of the Advanced Research WRF version 3". NCAR Technical note TN-475 + STR. Boulder, Colorado, USA, 113 pp., 2008.

Sun, S., Jin, J.M., and Xue, Y 1999. A simple snow-atmosphere-soil transfer model. J. Geophys. Res., 104, 19,587–19,597, doi: 10.1029/1999JD900305.

Yang Z.-L. and G.-Y. Niu 2003. The versatile Integrator of surface and atmospheric processes (VISA) part 1: Model description. Global Planet. Change, 38, 175–189, doi: 10.1016/S0921-8181(03)00028-6.

Yang, Z.-L., R. E. Dickinson, A. Robock, and K. Y. Vinnikov, 1997. Validation of the snow sub-model of the Biosphere-Atmosphere Transfer Scheme with Russian snow cover and meteorological observational data, J. Clim., 10, 353–373, doi:10.1175/1520-0442(1997)010<0353:VOTSSO>2.0.CO;2.